International Journal of Computer Science and Applications,
©Technomathematics Research Foundation
Vol. 13, No. 2, pp. 61 – 88, 2016

UML-RT HYBRID CONTROL STRATEGY APPROACH OF DC SERVOMOTOR ANGULAR SPEED BY USING AN EMBEDDED SLIDING MODE CONTROL

ROXANA-ELENA TUDOROIU†
Mathematics and Informatics, University of Petrosani, 20 Universiy Street, Petrosani, 332006, Romania
tudelena@mail.com

WILHELM KECS
Mathematics and Informatics, University of Petrosani, 20 Universiy Street, Petrosani, 332006, Romania
wwkecs@yahoo.com

MARIA DOBRITOIU
Mathematics and Informatics, University of Petrosani, 20 Universiy Street, Petrosani, 332006, Romania
mariadobritoiu@yahoo.com

NICOLAE ILIAS
Mechanical and Electrical Engineering, University of Petrosani, 20 Universiy Street, Petrosani, 332006, Romania
iliasnic@yahoo.com

The novelty of this paper is a hybrid approach for modeling and implementing a real-time control strategy of a dc Servomotor angular speed by using a sliding mode control module. The sliding mode controller is embedded in an open-loop control system structure with a dc Buck converter to stabilize and regulate the converter output voltage, despite the load current changes and unregulated power supply input voltage. The motivation of this approach is that the most of the physical objects from real life exhibit in a naturally way a hybrid structure, i.e. a switching continuous - discrete variable structure over the time. In our proposed embedded control system structure it is the dc Buck converter that exhibits a hybrid dynamics, modeled and implemented by using an academic evaluation version of software package AnyLogic 6.7. In addition the proposed hybrid real time control strategy proved their effectiveness among the formal languages, and through their use in different real time control systems industrial applications.

Keywords: UML-RT; hybrid control systems dynamics; AnyLogic hybrid simulator multiple-paradigm; sliding mode control; dc servomotor.

1. Introduction

Generally speaking a real time (RT) control system for it designs and implementation deals with two main concepts: the critical time and the timing constraints. Critical time constraints are associated with hard tasks, and the soft tasks are required to meet only the time constraints. Furthermore a real-time operating system (RTOS) provides the real-time system multitasking characteristics required for implementation: concurrency, parallelism, scheduling, and inter-task communication mechanism [Gambier, (2004)].

Bvd. Cetatii, Bloc 1/1, Sc:D, Ap. 10, Timisoara, Timis, Romania

The integrated architectures of the control systems are more complex, mostly having an embedded hybrid structure that requires a suitable modeling approach. In a simulation environment frame we found that AnyLogic multi-paradigm simulator is one of these suitable tools well documented in [Tudoroiu, (2012); Tudoroiu et al., (2015a); Tudoroiu et al., (2015b)]. The choice of the right formalism language is a critical issue met in any design and implementation of a highly complex control system that according to [Gambier, (2004)], it has to be identified in the early modeling process stage. Nowadays, the object-oriented (OO) modeling concept in software engineering, has become the most suitable modeling approach on a large scale for the applications using real time control systems [Selic and Rumbaugh (1998); Selic, (2000)]. Recently, the UML-RT becomes a world industry leader in software engineering control systems modeling. Its notation is useful to specify the requirements, document the structure, for object decomposition, as well as to define interactions between objects in a software system [Selic and Rumbaugh (1998); Selic, (2000)]. UML-RT is an extension of previous UML with additional modeling concepts, such as capsules, ports, connectors and protocols. The capsule represents the essential modeling block used in UML-RT. It is used to represent an active object inside a control system which can communicate as interface objects with other control system capsules or sub-capsules through ports [Selic, (2000)], [Tudoroiu, (2012); Tudoroiu et al., (2015a); Tudoroiu et al., (2015b)]. Figure 1 shows an example of a capsule structure diagram, represented in ROSE-RT editor, as in [Selic, (2000)], [Tudoroiu, (2012); Tudoroiu et al., (2015a); Tudoroiu et al., (2015b)]. More specifically, the UML-RT capsules are described using UML-RT graphical notations for class, collaboration and structure diagrams.

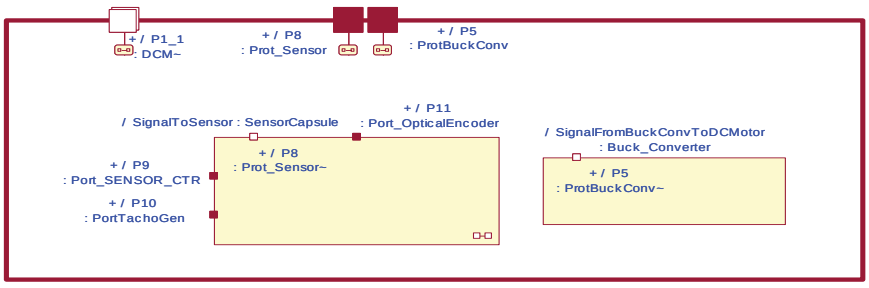

Fig. 1. Structure diagram with capsule composition, ports and protocol represented in Rose-RT editor (Reproduced from [Tudoroiu, (2012)]).

Each capsule or sub-capsule behavior is specified through a state machine. The state machine's trigger events are defined by the pair (port, signal), and the resulting action can be specified in Java code (AnyLogic) or other programming language. The ports are capsule's boundary objects through which the capsule can interact with its environment. In addition, the capsule and its ports have the same lifetime, i.e. a port instance owned by a capsule instance is created alongside with its capsule, and it is destroyed when its

capsule instance is destroyed [Selic, (2000)], [Tudoroiu, (2012); Tudoroiu et al., (2015a); Tudoroiu et al., (2015b)]. Also, a connector is a communication channel that exchanges the messages sent through the ports between parent and its immediate sub-capsules, as well as between sub-capsules.

2. Dc to Dc Buck Converter Hybrid Model State-Space Representation

The dc to dc buck converter is a power electronic component consisting of several switching electronic components, described by discontinuous differential equations, very difficult to model [Biswal, (2011)], [Tudoroiu, (2012)]. A dc to dc buck converter used in our research is a step-down dc converter, employed in a variety of industrial applications. The dc input of the converter is an unregulated dc voltage u, converted in a smaller regulated output voltage V_o, as shown in figure 2 [Biswal, (2011)], [Tudoroiu, (2012)]. In our experiment we use the dc to dc buck converter for simulation purpose, in order to prove the effectiveness of modeling the hybrid structure of the control systems by using the proposed hybrid simulator. Furthermore, the dc to dc buck converter is used to drive a dc servomotor that is connected in a feedback control loop together with a sliding mode control (SMC). For simulation purpose only two main variables are monitored in this integrated structure, namely the motor angular speed (ω) and its shaft angular position $(\theta(t) = d\omega/dt)$. A hybrid system consists of two main dynamics parts, namely a continuous part (System Dynamics), described by differential ordinary equations (ODEs) implemented by using the stock flow modeling concept of system dynamics (SD), known also as Forrester diagrams, and a discontinuous part that can be modeled by using the Discrete Event (DE) concepts, more precisely statecharts and finite state machines. We associate the operation modes to different states of the components of a power electronics hybrid system.

In figure 2, the dc buck converter consists of a MOSFET transistor switch Q (S_w), a freewheel diode D that reduces the dc component of voltage, and a low-pass filter that removes the high-frequency switching harmonics. The SWITCH S_w is controlled by a binary periodic signal CLOCK (t), of period T_s, and t_{on}, t_{off} representing the duration times for which the function values are equal to 1, and respectively to 0 [Biswal, (2011)], [Tudoroiu, (2012); Tudoroiu et al., (2015a); Tudoroiu et al., (2015b)]. The most important requirement for a dc converter is its high efficiency. The dc buck converter is equipped with a power MOSFET transistor and a diode. In addition, a trigger gate driver circuit switches the transistor Q between S_{on} and S_{off}, representing the conducting, respectively blocking states, commanded by a logic signal $\delta(t)$ [Biswal, (2011)]. The positive inductor current $i_L(t)$ flows through the MOSFET transistor, so $\delta(t)$ becomes lower at time $t = t_{on}$, thus commanding MOSFET Q to turn off. The inductor current must continue to flow; consequently, $i_L(t)$ forward biases the diode D, determining the output drain voltage (voltage dropped on the diode D) to be approximately equal to zero. Diode D conducts for the remainder of the switching period, such that the inductor current $i_L(t)$ remains positive; the diode D that operates in this manner is called freewheel diode.

Since the dc buck converter output voltage $V_o(t)$ is a function of the switch duty cycle, a control system can be implemented to vary the duty cycle (D) and to make its output voltage $V_o(t)$ in order to reach the value of a given reference voltage V_{ref}, as shown in the same figure 2.

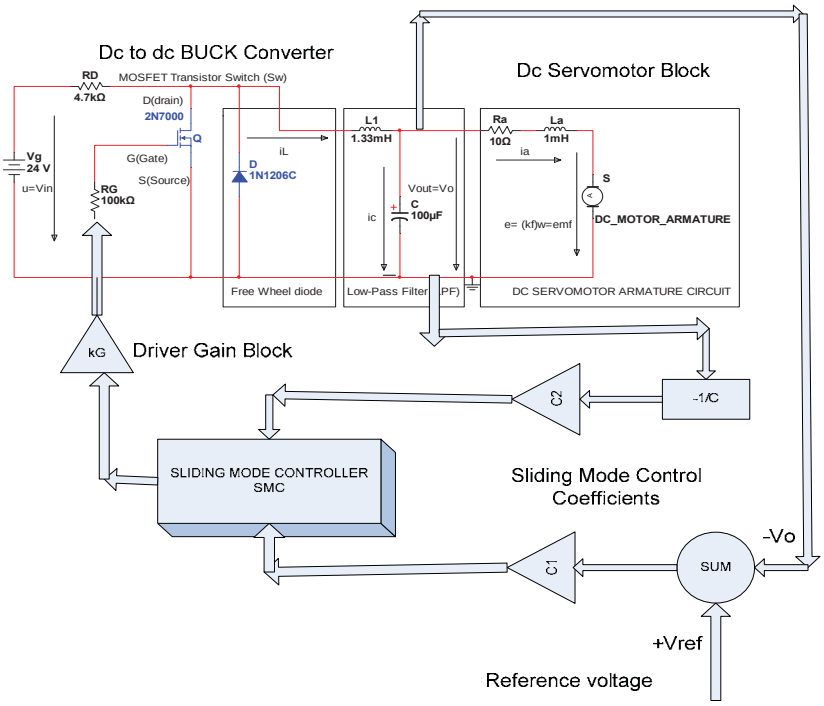

Fig. 2. The closed-loop control design using a sliding mode control (SMC) strategy to regulate the output voltage of the dc Buck converter (MULTISIM-11 and MICROSOFT VISIO design).

The both saturation (S_{on}) and blocking (S_{off}) states are simulated also using National Instruments software MULTISIM-11, as is shown in Figure 3.

The switch position varies periodically, making the output switch voltage a rectangular form wave, with period T_s and *duty cycle* $0 \le D \le 1$, representing the fraction of time for which the switch is connected in position 1 [Biswal, (2011)], [Tudoroiu, (2012); Tudoroiu et al., (2015a); Tudoroiu et al., (2015b)]. The switching frequency $f_s = 1/T_s$ usually lies in the range 1 kHz to 1 MHz, depending on the speed of the MOSFET devices. The output switch voltage waveform contains undesired harmonics caused by the switching frequency that are removed without power dissipation by LC low-pass filter section (assumed to be ideal), determining the continuous component of the dc buck converter output voltage V_{out}, to be effectively equal to that of

the switch dc component [Biswal, (2011)], [Tudoroiu, (2012); Tudoroiu et al., (2015a); Tudoroiu et al., (2015b)].

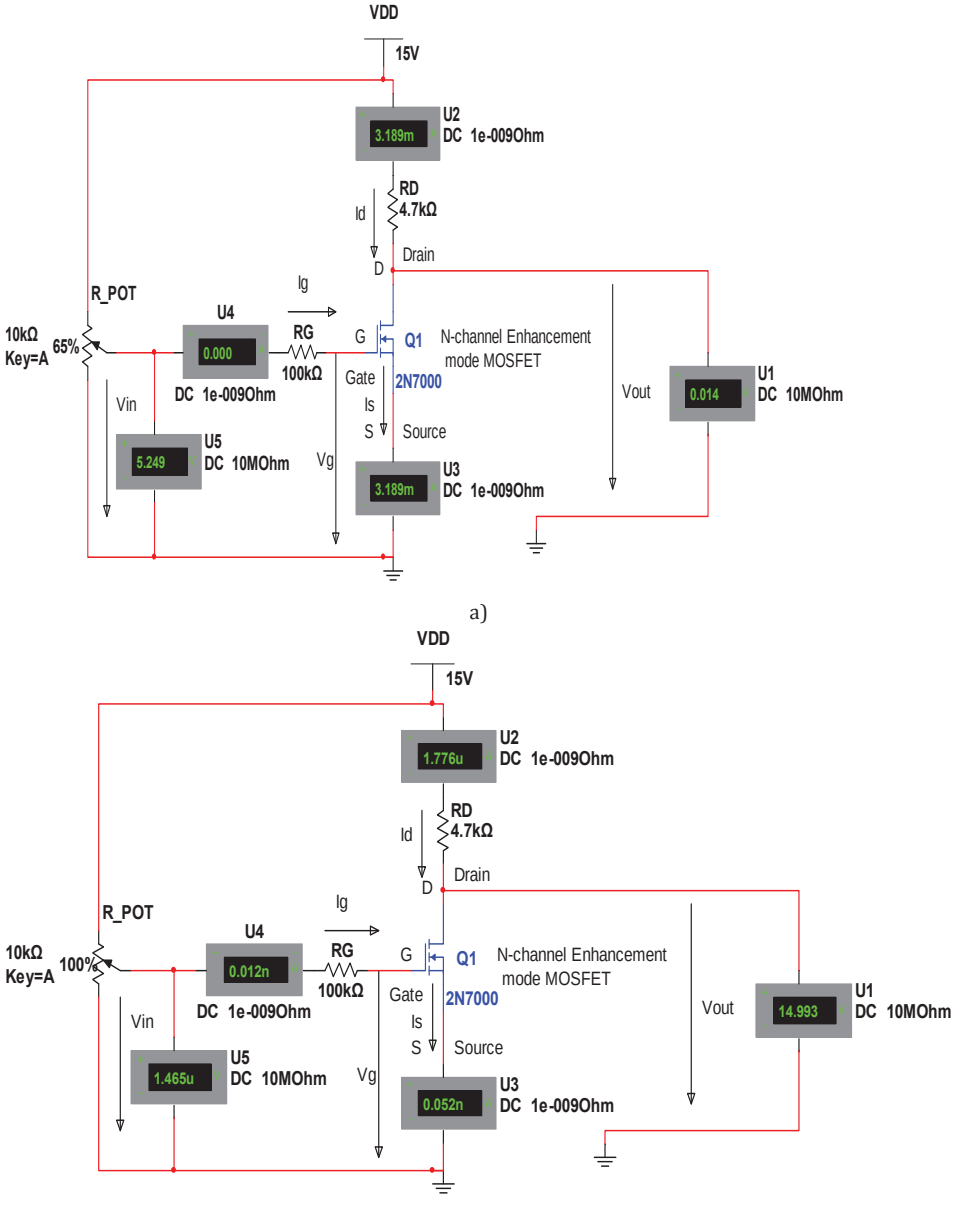

Figure 3: 2N7000 n-channel enhancement mode MOSFET transistor switching states: saturation (a) and blocking state (b)

The corner frequency of LC low-pass filter $f_c = 1/2\pi\sqrt{LC}$ is chosen to be sufficiently less than the switching frequency f_s in order to pass only the dc component of output switch voltage.

Concluding, the dc buck converter produces a dc output voltage controlled through the duty cycle *D* by using circuit elements that in an ideal situation do not dissipate energy [Biswal, (2011)], [Tudoroiu, (2012); Tudoroiu et al., (2015a); Tudoroiu et al., (2015b)]. In the next subsection we represent the time variable parameters hybrid structure of the dc buck converter dynamics under sliding mode control (SMC) described by a set of first order differential equations. The state machine of the dc buck converter capsule passes through three main states during its dynamic evolution, assigned to S_{on}, S_{off}, respectively S_{nc}, all these states being adapted to the overall control system design requirements. Furthermore, theirs meaning is more comprehensible in the following subsections where these states become visible in the statecharts. As input ports for dc buck converter capsule is considered the output voltage error, $x_1 = V_{ref} - v_0$ and the voltage error time variation, $x_2 = dx_1/dt$ (voltage error dynamics) [Biswal, (2011)], [Tudoroiu, (2012); Tudoroiu et al., (2015a); Tudoroiu et al., (2015b)].

2.1. *Dc to dc buck converter capsule dynamics in continuous control mode operation (CCM)*

- The discrete state S_{on} corresponds to the closed position of the switch S_w such that the diode is staying reverse biased.

The dynamics of dc buck converter electrical circuit, without diode and with the switch S_w set on closed position in Continuous Control Mode (CCM) operation is determined by a current i_L flowing through the coil continuously and is described in state-space representation by the following equations [Biswal, (2011)], [Tudoroiu, (2012); Tudoroiu et al., (2015a); Tudoroiu et al., (2015b)]:

$$\begin{aligned} \frac{dx_1}{dt} &= -\frac{1}{L}x_2 + \frac{1}{L}u = a_{11}x_1 + a_{12}x_2 + b_1u \\ \frac{dx_2}{dt} &= -\frac{1}{C}x_1 - \frac{1}{RC}x_2 = a_{21}x_1 + a_{22}x_2 + b_2u \\ y &= x_2,\ \mathrm{x_1 = i_L, x_2 = v_C, u = V_g}. \end{aligned} \tag{1}$$

- The state S_{off} corresponds to an opening switch position S_w that determines the inductor current $i_L(t)$, whenever it is positive, to flow through the forward biased diode D. Therefore, the diode can be replaced by a conductor of zero resistance, becoming a short-circuited diode branch. In this case the switch and so the power supply input source voltage, *u*, are short-circuited by the diode branch, thus eliminated during dc analysis. Also, in our development we assume an ideal case, ignoring completely the almost 0.7 V diode dropped voltage.

Furthermore, the state S_{off} still remains in continuous control mode (CCM), such that its hybrid structure dynamics can be described by similar first order differential equations obtained by replacing in (1) $u = 0$ (S_w opened) [Biswal, (2011)], [Tudoroiu, (2012); Tudoroiu et al., (2015a); Tudoroiu et al., (2015b)]:

$$\begin{aligned} \frac{dx_1}{dt} &= -\frac{1}{L}x_2 = a_{11}x_1 + a_{12}x_2 + b_1u \\ \frac{dx_2}{dt} &= -\frac{1}{C}x_1 - \frac{1}{RC}x_2 = a_{21}x_1 + a_{22}x_2 \\ y &= x_2,\ x_1 = i_L, x_2 = v_C, u = 0. \end{aligned} \tag{2}$$

2.2. *Dc to dc buck converter capsule dynamics in discontinuous control mode operation (DCM)*

- The state S_{nc} occurs when the switch is set in switch-off mode and $i_L > 0$ monotonically decreases due to the self-induction effect; also, the capacitor voltage v_c increases since the capacitor is in charging cycle [Biswal, (2011)], [Tudoroiu, (2012); Tudoroiu et al., (2015a); Tudoroiu et al., (2015b)]. Moreover, if the time is long enough for the charging cycle, there exists a time instant when the coil current is cancelled and the capacitor is trying unsuccessfully to discharge through the diode, consequently $i_L = 0$.

The dynamics of the hybrid discrete structure in discontinuous control mode operation (DCM) is described by similar equations obtained by replacing $u = 0$ (S_w opened) in (1), and also $i_L = 0$:

$$\begin{aligned} \frac{dx_1}{dt} &= 0 = a_{11}x_1 + a_{12}x_2 + b_1u \\ \frac{dx_2}{dt} &= -\frac{1}{RC}x_2 = a_{21}x_1 + a_{22}x_2 + b_2u \\ y &= x_2, x_1 = 0, x_2 = v_C, u = 0. \end{aligned} \tag{3}$$

An advantage of this description is the fact that the model of the first operation mode S_{on} could be reused to determine the model for the other two operating modes S_{off}, respectively S_{nc}. AnyLogic Editor Properties offers this facility by changing easily the trigger values u, and also $dx_1/dt = 0$ [Tudoroiu, (2012); Tudoroiu et al., (2015a); Tudoroiu et al., (2015b)].

2.3. *Using AnyLogic hybrid simulator to model and implement the dc to dc buck converter dynamics*

The equations (1)-(3) describing the dynamics of the dc buck converter are in the standard explicit form, easily to translate the right hand side of the differential equations into AnyLogic Forrester diagrams. Also, the corresponding values of dc buck converter

states are assigned into AnyLogic editor to the state actions. Closing, the hybrid state transitions and the parameters of the states S_{on}, S_{off}, S_{nc} correspond to (CCM) and (DCM) modes and are assigned to the transitions and parameters in AnyLogic hybrid simulator in a straightforward way [Tudoroiu, (2012); Tudoroiu et al., (2015a); Tudoroiu et al., (2015b)]. In our development we choose for dc buck converter capsule the following statechart features (AnyLogic -Statechart Palette's editor):

- Entry actions:

S_{on} – entry action: $a_{11} = 0, a_{12} = -\frac{1}{L}, a_{21} = -\frac{1}{C}, a_{22} = -\frac{1}{RC}, b_1 = \frac{1}{L}, b_2 = 0$

S_{off} – entry action: $a_{11} = 0, a_{12} = -\frac{1}{L}, a_{21} = -\frac{1}{C}, a_{22} = -\frac{1}{RC}, b_1 = 0, b_2 = 0$

S_{nc} – entry action: $a_{11} = 0, a_{12} = 0, a_{21} = 0, a_{22} = -\frac{1}{RC}, b_1 = 0, b_2 = 0.$

- Triggered Transitions:

$S_{on} - S_{off}$ - Transition triggered timeout = t_{on}
$S_{off} - S_{on}$ - Transition triggered by timeout = T_s
$S_{off} - S_{nc}$ - Transition triggered by condition: $i_L \leq 0$
$S_{nc} - S_{on}$ - Transition triggered by timeout = T_s

In AnyLogic editor we model all these states by using Forrester diagram (SD part) and Statechart (DE part), for the following values of the parameters [Tudoroiu, (2012); Tudoroiu et al., (2015a); Tudoroiu et al., (2015b)]:

$$T_s = 0.001[s], t_{on} = 0.4T_s, u = 24\ [\mathrm{V}], R = 8[\Omega], L = 0.00133\ [H], \mathrm{C} = 0.0001[F],$$

corresponding to the tuning values for the electrical circuit shown in figure 2, with the dc servomotor and the sliding mode control disconnected; the armature of the dc servomotor is replaced by the $8[\Omega]$ resistance R. The model and the simulation results are presented in figures 4-5, for the both CCM states S_{on}, respectively S_{off}.

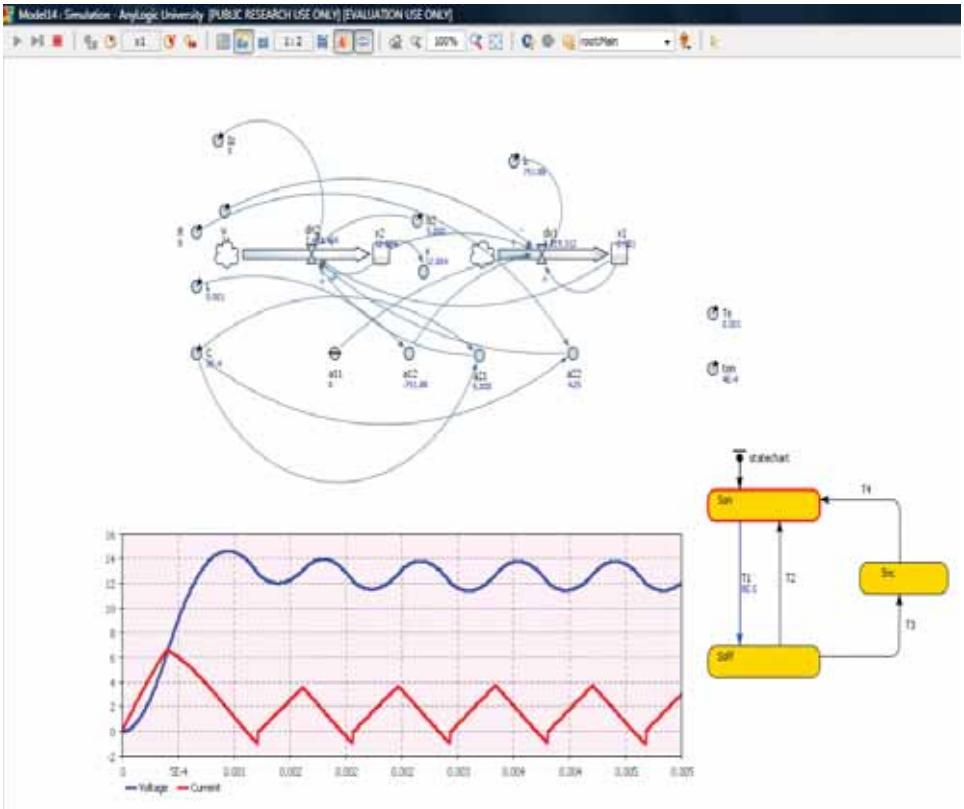

Fig. 4. Forrester diagram of dc to dc buck converter model and statechart simulations-The hybrid structure is in the first state, S_{on} (Reproduced from [Tudoroiu, (2012); Tudoroiu et al., (2015a); Tudoroiu et al., (2015b)])

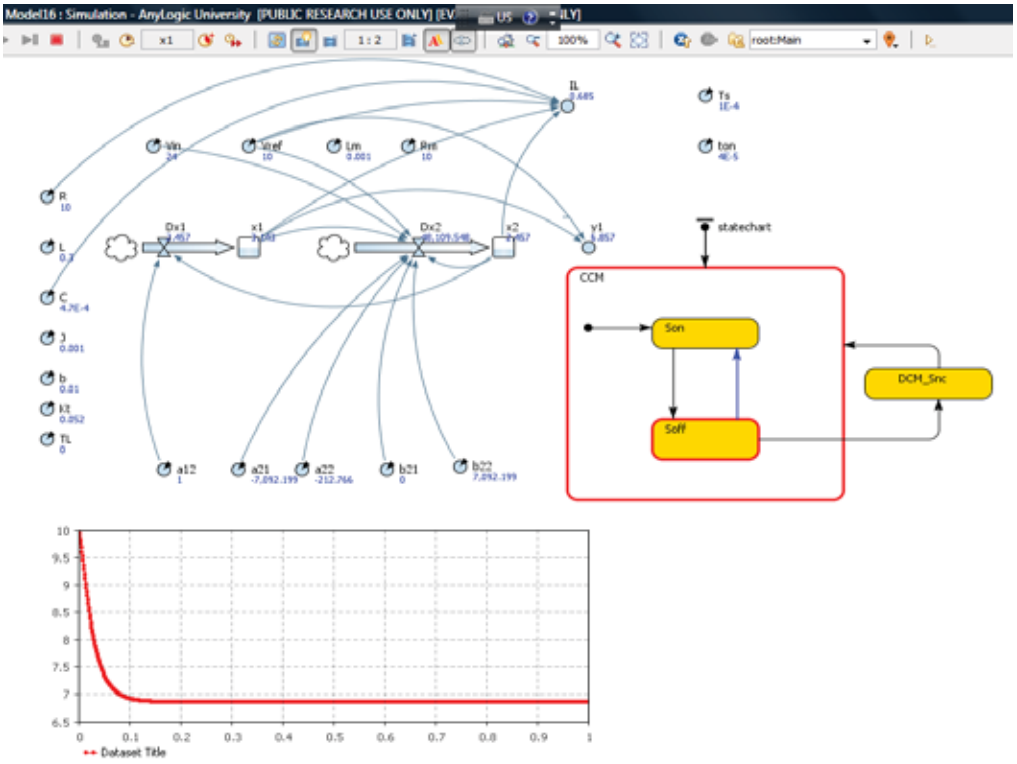

Fig. 5. Forrester diagram of dc to dc Buck converter model and statechart simulations-The hybrid structure is in the second state, $\boldsymbol{S_{off}}$(Reproduced from [Tudoroiu, (2012); Tudoroiu et al., (2015a); Tudoroiu et al., (2015b)]).

3. DC Servomotor Capsule Dynamics Modeling and Implementation - Anylogic versus MATLAB/SIMULINK

The dc servomotor is mostly used as an actuator in feedback closed-loop control systems, but in this research for simulation purposes it is design as a controlled plant. The main goal of the overall proposed control strategy is to control its angular speed or its position, or the both. Consequently, the dc servomotor component becomes a new capsule in the hybrid control system with its integrated structure represented in figures 6-7. The links between all three capsules (dc Servomotor, dc Buck converter and Controller block) in the integrated structure are performed by mean of the input and output ports. Compared to dc buck converter the dc servomotor capsule has only continuous dynamics. For simulation purpose, in order to prove the effectiveness of our proposed hybrid control strategy we investigate a 24 V dc servomotor with similar electrical and mechanical characteristics as in [Tudoroiu, (2012); Tudoroiu et al., (2015a); Tudoroiu et al., (2015b)]:

- moment of inertia of the rotor: $J = 0.001\ [\frac{kgm^2}{s^2}]$

- damping ratio of the mechanical system: $B_m = 0.01[Nms]$

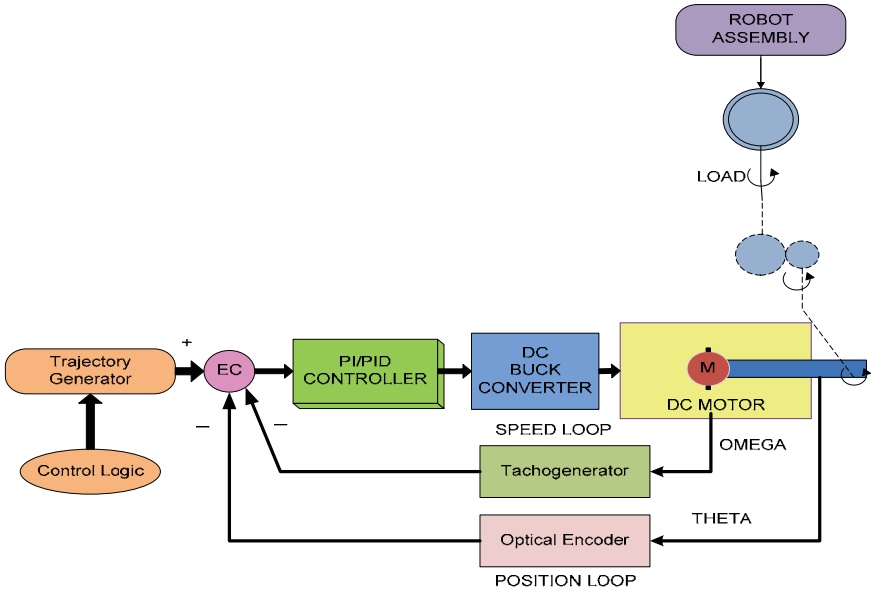

Fig. 6. The feedback closed-loop control system of the dc servomotor angular speed OMEGA (ω) and angular position THETA (θ)- schematic diagram (Reproduced from [Tudoroiu, (2012)]).

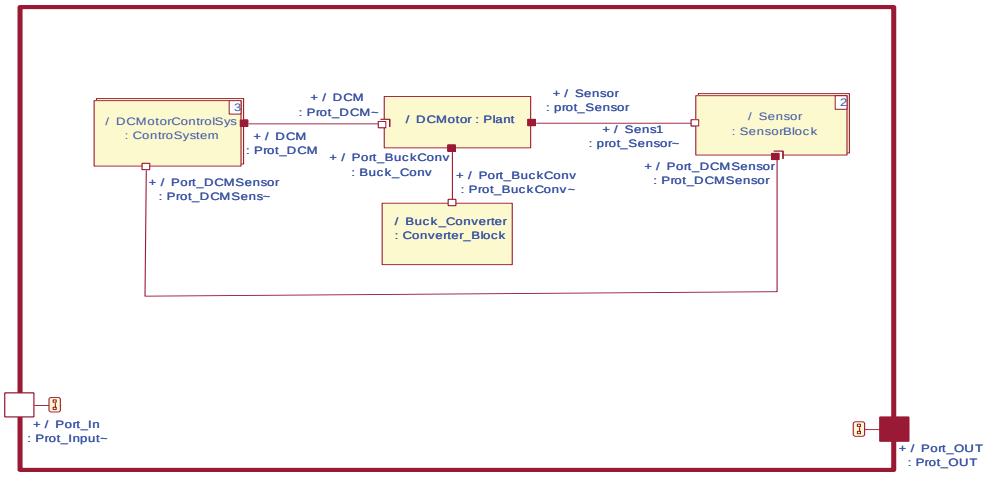

Fig. 7. UML – collaboration diagram represented in ROSE-RT editor (Reproduced from [Tudoroiu, (2012); Tudoroiu et al., (2015a); Tudoroiu et al., (2015b)])

- electromotive force constant: $k_t = k_e = 0.0517\ [Nm/A]$
- motor electric resistance *:* $R_a = 10\ [\Omega]$

- motor electric inductance :$L_a = 0.001[H]$
- the field-armature mutual inductance $L_{af} = 1.8[H]$
- initial speed $\omega = 1[\frac{\text{rad}}{\text{s}}]$,

closed enough to those derived by experiment from an actual motor in Carnegie Mellon's control lab of the University Michigan [Tudoroiu, (2012)]. The equivalent electrical schematic of the selected dc servomotor is presented in MULTISIM-11 as shown in figure 8, and its SIMULINK model is also represented in figure 9.

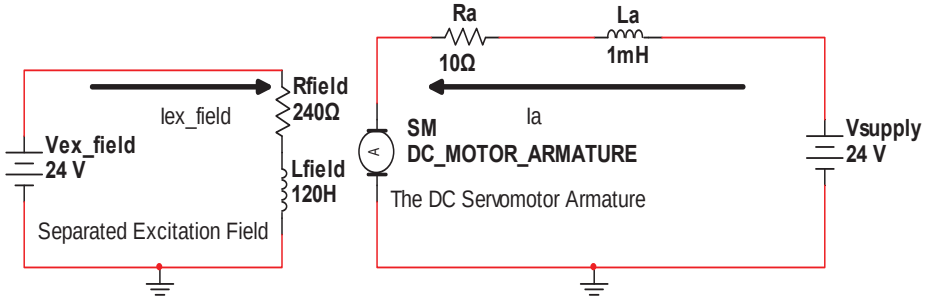

Fig. 8. The equivalent electrical schematic of dc servomotor designed in MULTISIM-11

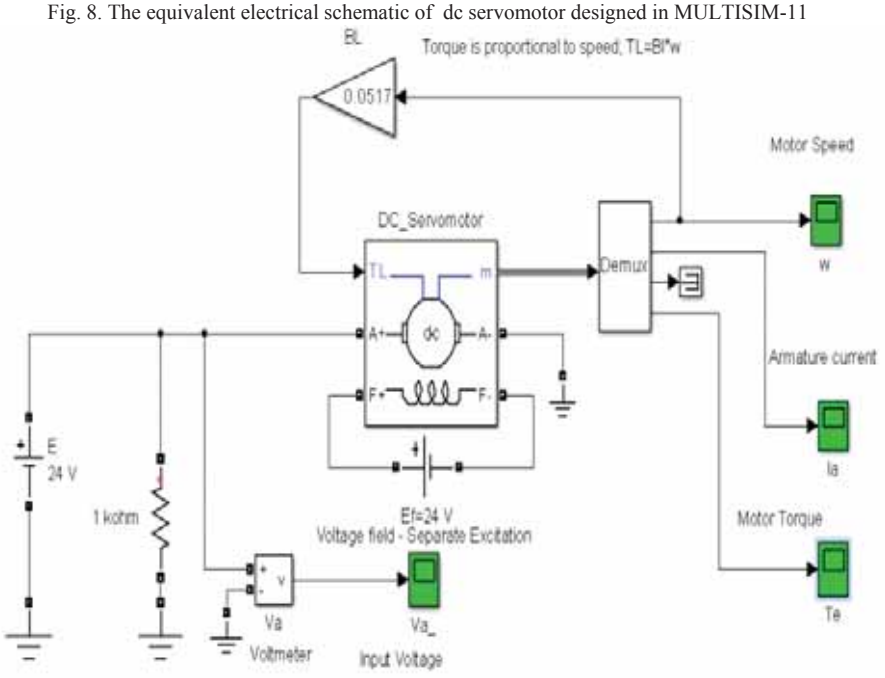

Fig. 9. The SIMULINK model of the selected dc servomotor capsule

Furthermore, the simulation results of the SIMULINK model of dc servomotor dynamics are shown in figures 10-12, and for simplicity model purpose it is assumed that the rotor and the shaft of dc servomotor are rigid.

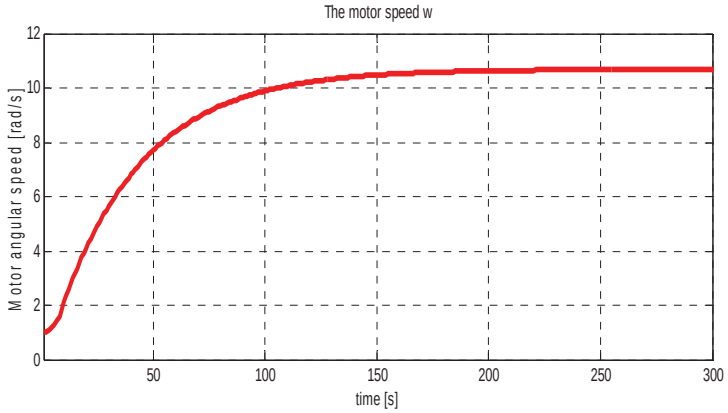

Fig. 10. The dc servomotor speed response - SIMULINK simulation results

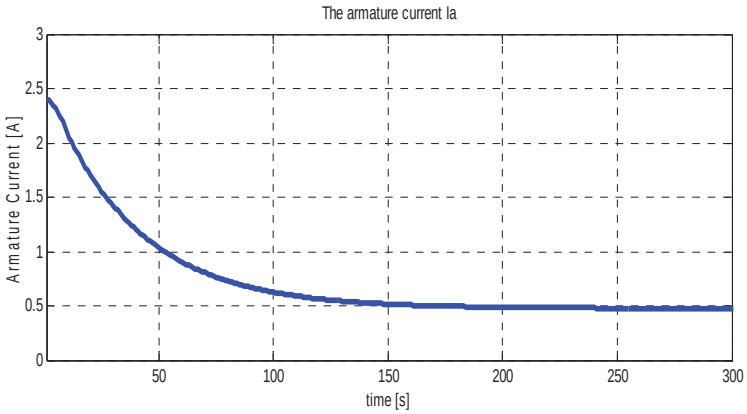

Fig.11.The dc servomotor armature current - SIMULINK simulation results

The dynamics of the dc servomotor capsule is described by following differential equations [Tudoroiu, (2012); Tudoroiu et al., (2015a); Tudoroiu et al., (2015b)]) :

$$J\frac{d^2\theta}{dt^2} + B_m\frac{d\theta}{dt} = k_t I_a - T_L$$
$$L_a\frac{dI_a}{dt} + R_a I_a = V_1 - k_e\frac{d\theta}{dt}\,. \tag{4}$$

where $T_e = k_t I_a$ is the torque generated by the dc servomotor, T_L is the torque load, and $e = k_e\frac{d\theta}{dt} = k_e\omega$ is the counter electromotive force (*cef*) of the dc servomotor, $\mathrm{k_e}$ representing the counter electromotive force coefficient.

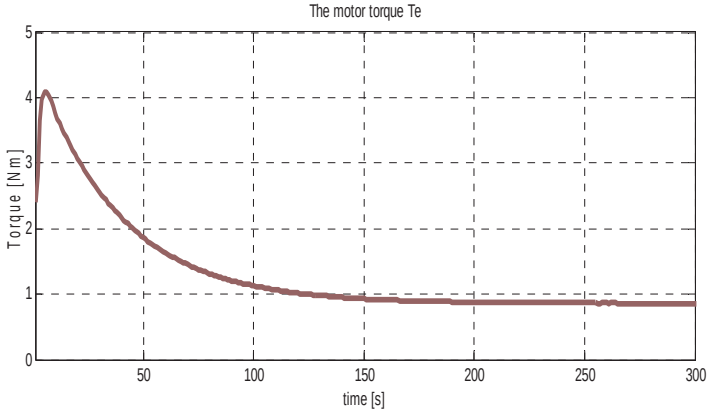

Fig. 12. The dc servomotor motor torque SIMULINK simulation results

By replacing $\omega = \frac{d\theta}{dt}$ in previous equations (4) that represents the link between angular speed (ω) and angular position(θ), the dc servomotor dynamics is described by a standard second order differential equation:

$$JL_a \frac{d^2\omega}{dt^2} + 2\zeta\omega_n \frac{d\omega}{dt} + \omega_n^2\omega = k_m u \tag{5}$$

where

$$y = \omega, u = V_1,\ \omega_n = \sqrt{\frac{R_a B_m + k_t^2}{JL_a}}, \zeta = \frac{B_m L_a + JR_a}{2\sqrt{JL_a(R_a B_m + k_t^2)}}, k_m = \frac{k_t}{JL_a}, \tag{6}$$

- ω_n represent the natural frequency of the free oscillations, ζ the damping factor, and k_m is the dc servomotor gain.

Using the set up numerical values of electrical and mechanical parameters of our proposed dc servomotor machine we get the following dc servomotor transfer function representation:

$$H(s) = \frac{k_m}{s^2 + 2\zeta\omega_n s + \omega_n^2} = \frac{Y(s)}{U(s)} = \frac{51700}{s^2 + 10010s + 102670} \tag{7}$$

where s represents the equivalent of the derivative operator in complex domain, and $U(s), Y(s)$ represent the Laplace images of u(t) (input voltage) and $y(t)$ (output voltage), respectively. In MATLAB simulations environment the equation (5) is modeled by using MATLAB step function provided by CONTROL SYSTEMS MATLAB TOOLBOX. The simulation results are shown in figure 13 for dc servomotor angular speed, that are closed enough with those obtained in SIMULINK simulations, depicted in figure 10. We can see easily that the steady state value of the dc servomotor angular speed is approximately 12 [*rad/s*] in the both cases.

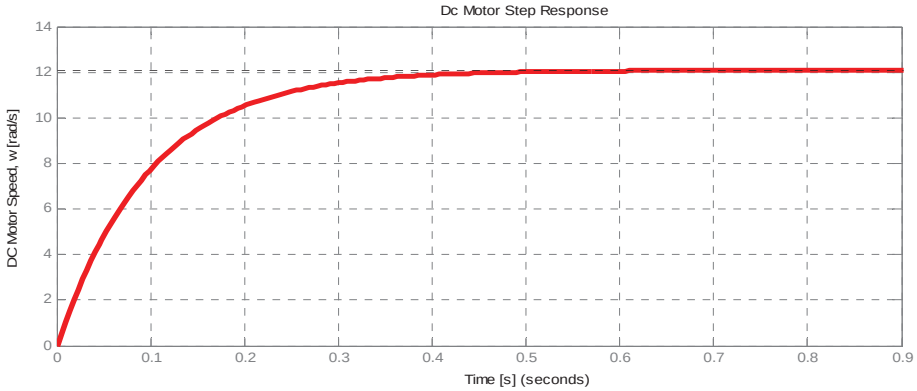

Fig. 13. The dc servomotor speed step response MATLAB simulation results

For comparison purpose we show also the simulation results of the dc servomotor capsule step response in AnyLogic hybrid simulator, such as shown in figure 14, based on the dynamics described by (5), (7) or (8), written in a state-space representation:

$$\frac{dx_1}{dt} = x_2$$
$$\frac{dx_2}{dt} = -\omega_n^2 x_1 - 2\zeta\omega_n x_2 + k_m u \tag{8}$$
$$x_1 = \omega, x_2 = \frac{d\omega}{dt}, y = x_1$$

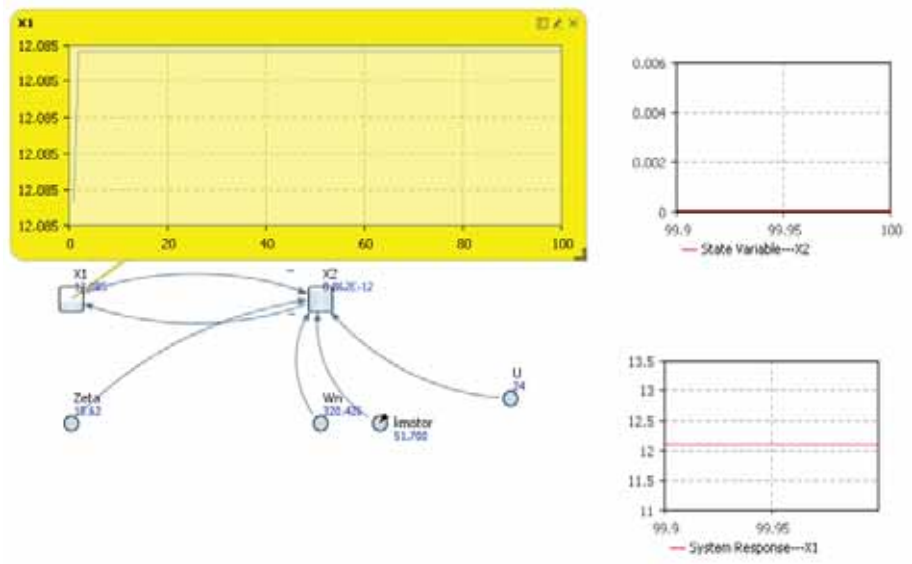

Fig. 14. Forrester diagram (dynamic model) of dc servomotor angular speed simulation results in AnyLogic hybrid simulator (PLE free evaluation version snapshot)

4. Integrated Capsules Structure - Model Dynamics and Implementation using Anylogic Hybrid Simulator

The dc servomotor capsule is embedded in open-loop control structure together with a dc buck converter capsule that provides a regulated input voltage. The dc servomotor has good speed control response, extensive control range, mainly used in speed control systems that need high control design requirements. To control the speed smoothly, the technique mostly used is to adjust the motor armature voltage [Tudoroiu, (2012); Tudoroiu et al., (2015a); Tudoroiu et al., (2015b)]. One of the most common methods used to drive a dc servomotor is to use the PWM signals with respect to dc servomotor input voltage, but the basic hard switching strategy causes unsatisfactory dynamic behaviour since the resulting trajectories reveal a very noisy shape [Tudoroiu, (2012); Tudoroiu et al., (2015a); Tudoroiu et al., (2015b)]. Consequently, this technique might cause large forces acting on the servomotor mechanics. Also, large currents (faulty currents) destructively stress the electronic components of the dc servomotor, and high failure risks of power supply possibly will take place.

The simplified model of the overall control system loop consisting of dc buck-converter driven a dc servomotor is shown in figure 15 [Tudoroiu, (2012); Tudoroiu et al., (2015a); Tudoroiu et al., (2015b)]. In this schematic, the switching devices have been replaced by an ideally switched voltage source, indicated by the multiplication of the input voltage source u with the switching variable δ, and also for consistency of our notation it will be considered the duty cycle variable D. The dc servomotor can be modeled by an inductance L_a (with ohmic resistance R_a) and an electromagnetic voltage source (electromotive force, *emf*). An input voltage u that equals the maxim voltage of the dc servomotor is also considered. The dc servomotor component of the control loop under our considerations is assumed to act on a generic manipulator robot arm.

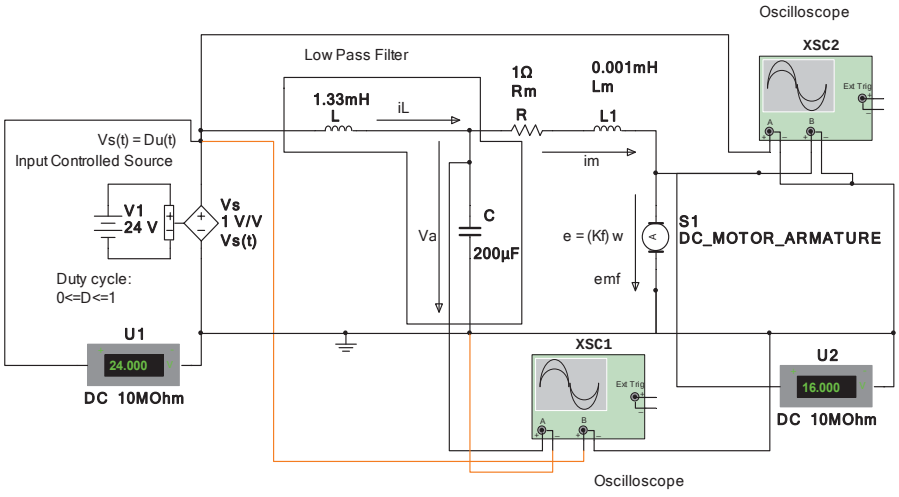

Fig. 15. The schematic of dc buck converter driving a dc servomotor (Multisim-11 Simulation Tool, Reproduced from [Tudoroiu, (2012); Tudoroiu et al., (2015a); Tudoroiu et al., (2015b)])

In addition, the values of dc buck converter parameters are the same as those used in the previous simulations or preliminary results (performed in AnyLogic environment) [Tudoroiu, (2012); Tudoroiu et al., (2015a); Tudoroiu et al., (2015b)] , namely:

- Low pass filter parameters: $L = 0.133$ [H], $C = 200$ [μ F], $u\ (V_g) = 24$ [V],
- Converter switching period $T_s = 0.001$[s], $t_{on} = 0.0004$ [s],
- Duty cycle $D = 0.4$.

The emerged dc to dc buck converter dynamics is described by the following equations:

$$\begin{gathered}\frac{dx_1}{dt} = -\frac{1}{L}x_2 + \frac{1}{L}Du(t) \\ \frac{dx_2}{dt} = \frac{1}{C}x_1 - \frac{1}{C}i_m \\ y = x_2,\ \mathrm{x_1} = \mathrm{i_L}, \mathrm{x_2} = \mathrm{v_C}, D\mathrm{u} = \mathrm{V_s}.\end{gathered} \tag{9}$$

where i_m is the armature current value of the dc servomotor.

It is worth also to mention that in all our simulations the load dc servomotor torque T_L is considered applied as a series input disturbance to the dc servomotor actuator block.

This assumption is useful to create one of the control event scenario for proposed dc servomotor functionality by generating the HALT state, related to situation when the dc servomotor torque developed to the shaft T_e is smaller than load torque T_L.

The dynamics of the hybrid structure will be given by the same set of differential equations (2)-(4) completed with the dc servomotor dynamics, as following [Tudoroiu, (2012); Tudoroiu et al., (2015a); Tudoroiu et al., (2015b)]:

- S_{on} dc to dc buck converter equations (1) and,

$$\begin{gathered}\frac{dx_3}{dt} = x_4 \\ \frac{dx_4}{dt} = -\omega_n^2 x_3 - 2\zeta\omega_n x_4 + k_m u \\ x_3 = \omega, x_4 = \frac{d\omega}{dt}, y = x_3.\end{gathered} \tag{10}$$

- S_{off} dc to dc buck converter equations (2) and,

$$\begin{gathered}\frac{dx_3}{dt} = x_4 \\ \frac{dx_4}{dt} = -\omega_n^2 x_3 - 2\zeta\omega_n x_4 + k_m u \\ x_3 = \omega, x_4 = \frac{d\omega}{dt}, y = x_3.\end{gathered} \tag{11}$$

- S_{nc} dc to dc buck converter equations (3) and,

$$\frac{dx_3}{dt} = x_4$$

$$\frac{dx_4}{dt} = -\omega_n^2 x_3 - 2\zeta\omega_n x_4 + k_m u \tag{12}$$
$$x_3 = \omega, x_4 = \frac{d\omega}{dt}, y = x_3.$$

where ω_n, and ζ are given by (6).

For this combined system structure (dc buck converter - dc servomotor) the event transitions from one state to another state could be built by using trigger events driven by u_1, x_1. The hybrid integrated structure of these two capsules is described by similar entry actions and triggered transitions as for dc to dc buck converter, developed in second chapter. The hybrid model and the system response simulation results in AnyLogic hybrid simulator for the combined structure and no-load conditions ($T_L = 0$) are shown in figure 16, where for readability purpose we show the AnyLogic model and the simulations results separately. In the Editor statechart are shown on the same diagram the dc servomotor speed response,ω the dc servomotor current,i_m and Low Pass Filter output voltage. This diagram and the experimental setup reveal that the no-load dc servomotor speed reaches steady-state value (100 rad/s) very fast (almost 2 seconds rise time, and 4 seconds settling time) without oscillations or overshoot, so a very good performance [Tudoroiu, (2012); Tudoroiu et al., (2015a); Tudoroiu et al., (2015b)].

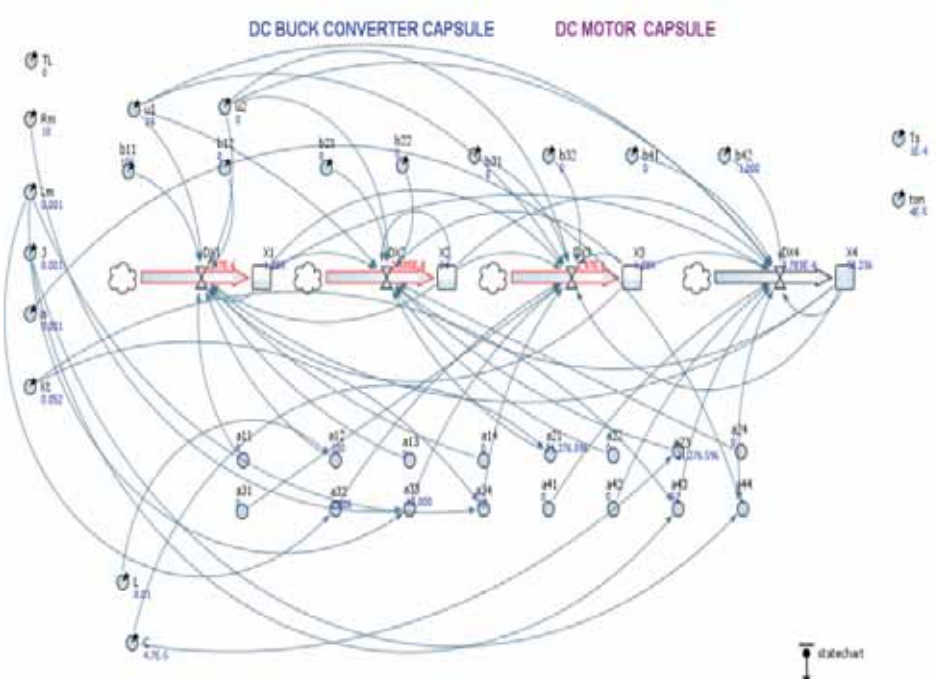

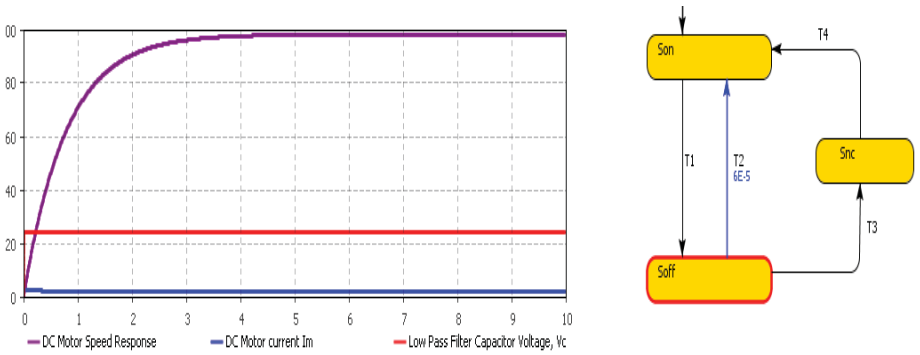

Fig. 16. Combined buck converter and dc servomotor open-loop control system model and system response - simulation results in AnyLogic 6.7 University (Free evaluation version) - Hybrid approach (no-load case, $T_L = 0$ Nm, (Reproduced from [Tudoroiu, (2012); Tudoroiu et al., (2015a); Tudoroiu et al., (2015b)]).

The load effect can be seen in figure 17, for T_L = 0.1Nm. The simulation results reveal that the dc servomotor speed becomes negative; perhaps the motor torque (Te) is less than load torque (T_L).

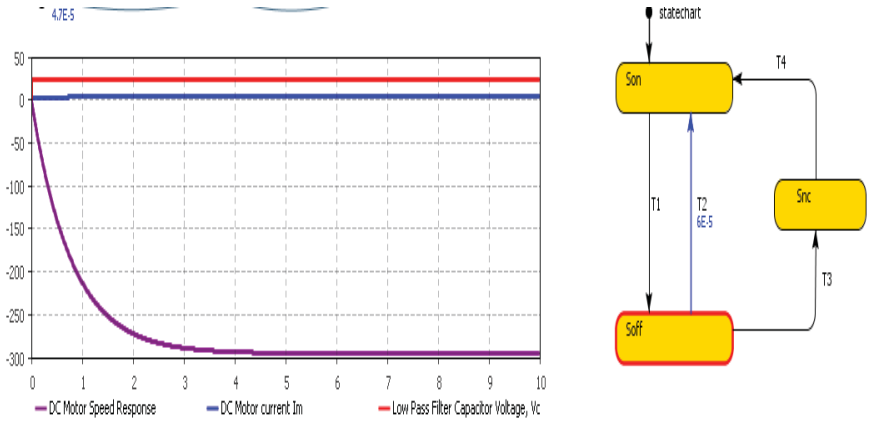

Figure 17: The load effect of the combined Buck converter and dc servomotor open-loop control system - simulations results in AnyLogic6 hybrid simulator (T_L = 0.5 [Nm], (Reproduced from [Tudoroiu, (2012); Tudoroiu et al., (2015a); Tudoroiu et al., (2015b)]).

Closing, for an embedded open-loop control structure (dc buck converter – dc servomotor) during modelling phase it must be implemented all the situations possible, so we have to enlarge the number of discrete event states from three to seven, three states for dc buck converter (S_{on}, S_{off}, S_{nc}) and four states for dc servomotor (STOP, START,

HALT, FAIL), defined as follows [Tudoroiu, (2012); Tudoroiu et al., (2015a); Tudoroiu et al., (2015b)]:
START – is the normal working state of the dc servomotor under nominal conditions (no-load nominal speed, nominal current and power supply voltage as well as the active power absorbed)
STOP – is the rest position state of the dc servomotor
HALT – is the state that occurs when the servomotor torque is less than load torque, $T_e < T_L$. This could be a dangerous situation since the current could build up in the coils (armature, stator) that can damage the dc servomotor. Usually in this situation the motor has to be rapidly disconnected from the power supply source, so the motor passes in STOP state.
FAIL – is an abnormal situation created by the excessive increasing of the dc servomotor current or viscous friction in the servomotor bearings (current and friction faults).

4.1. *RT combined structure control strategy of angular speed and dc servomotor position in open-loop-hybrid approach*

The dynamic equations of each possible discrete state ($\mathrm{S_{on}}, \mathrm{S_{off}}, \mathrm{S_{nc}}$) of the hybrid combined structure will be completed with a new differential first order equation that relates the servomotor speed (ω) and its shaft position (θ) [Tudoroiu, (2012); Tudoroiu et al., (2015a); Tudoroiu et al., (2015b)]:

$$\omega = \frac{d\theta}{dt} \tag{13}$$

The model implemented in AnyLogic and the system response simulation results are shown in figure 18. Due to the fact that the angular speed becomes constant very fast, and also it is positive, the position will be linear monotonically increasing. The dc servomotor is also loaded, assuming a load torque T_L = 0.001 [Nm] [Tudoroiu, (2012); Tudoroiu et al., (2015a); Tudoroiu et al., (2015b)].

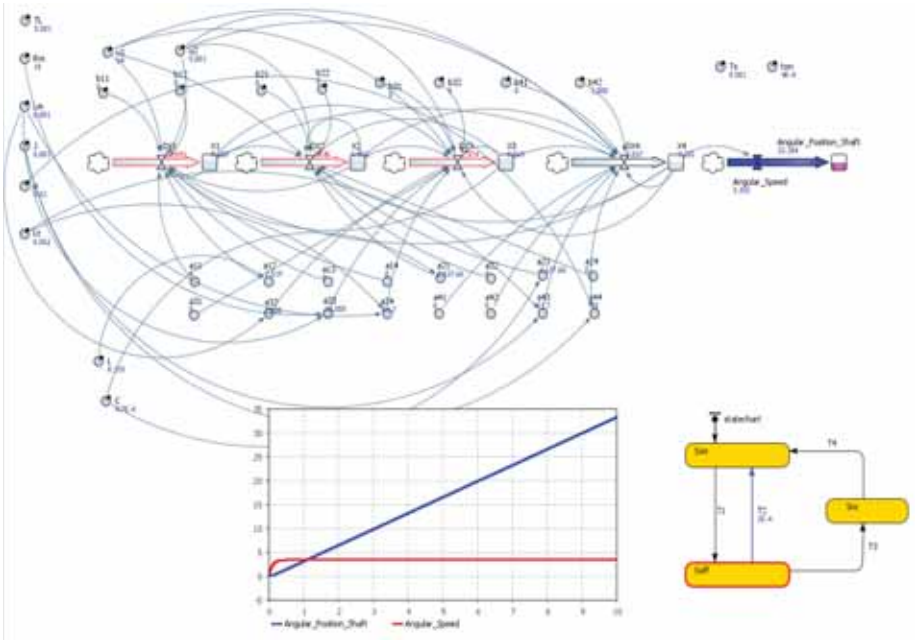

Fig. 18: Open-loop dc servomotor angular speed (red curve) and its corresponding angular position (blue line) in the embedded structure (Reproduced from [Tudoroiu, (2012); Tudoroiu et al., (2015a); Tudoroiu et al., (2015b)]).

5. Sliding Mode Control

In a hybrid control system approach, described by a switching dynamics between three states (S_{on}, S_{off}, S_{nc}), a sliding mode control (SMC) strategy is more suitable to perform better than a standard PID control strategy. This is a natural way approach, taking into consideration the particular dynamics captured by the hybrid control system. Compared to another control strategies, the sliding mode control (SMC) is more robust, very easy to implement, performs with a good dynamic response and stability due to its robustness to parameters changes [Biswal, (2011)], [Tudoroiu, (2012)]. The basic idea of sliding mode control (SMC), as shown in figures 19-20, resides in designing firstly of a sliding surface in state-space, and then to design a control law through the system state trajectory starting from any arbitrary initial state to reach the sliding surface in finite time, and finally it should converge to an equilibrium point (usually, the origin point of the phase plane) [Biswal, (2011)], [Tudoroiu, (2012)].

Therefore the existence, stability and hitting condition are three factors for the stability of sliding mode control (SMC). The basic principle of the sliding mode control is well documented in [Biswal, (2011)], [Tudoroiu, (2012)], and depicted with additional details in figure 19, to have a good insight of the phenomenon involved in switching dynamics of this particular control system strategy.

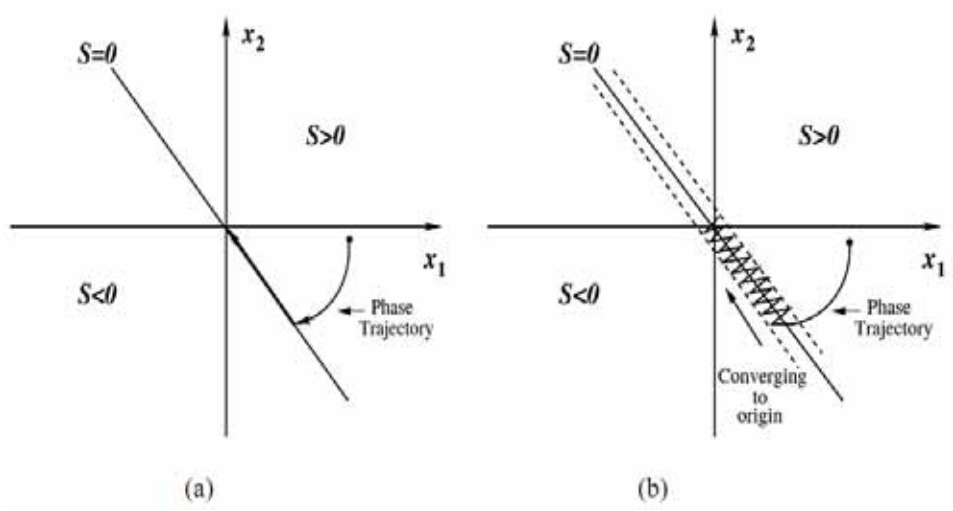

Fig. 19. Switching dynamics represented in phase plane for: (a) ideal sliding mode control and (b) practical sliding control mode (Reproduced from [Biswal, (2011)], [Tudoroiu, (2012)])

In figure 19 x_1 represents the voltage and x_2 is the voltage rate, and the plane delimited by these two phase variables is known as the phase plane.

In this plane (x_1, x_2), S(x_1, x_2, t) = 0 represents the sliding surface, and the sliding line divides the phase plane into two regions, specified each one with its own switching state [Biswal, (2011)], [Tudoroiu, (2012)]. When the trajectory converges to the system equilibrium point, as a solution of the following equations:

$$\frac{dx_1}{dt} = 0$$
$$\frac{dx_2}{dt} = 0 \tag{14}$$

where $x_2 = \frac{dx_1}{dt}$.

and the system is considered stable, otherwise is unstable (divergent). Also, if the hysteresis band around the sliding line becomes zero, then the system is operating with an ideal SMC, but in reality this situation never happens to be achieved, the control system having a finite switching frequency [Biswal, (2011)], [Tudoroiu, (2012)]:

$$f_s = \frac{1}{T_s}. \tag{15}$$

To control the angular speed or the angular position of the dc servomotor firstly it must to design a closed-control loop by using a SMC strategy, as those shown in figure 2. The dc servomotor dynamics is described by the following equation [Biswal, (2011)], [Tudoroiu, (2012)]:

$$L_a \frac{di_a}{dt} + R_a i_a + k_e \omega = v_0 \, . \tag{16}$$

The loop input is considered the dc buck converter input voltage, $u = \mathrm{v_g}$, a discontinuous variable with its value depending of the switch position, S_w. Therefore, the dc buck converter behaviours as a time variable and a nonlinear switch with variable structure features. The SMC uses a sliding surface to decide its input states to the control system. The switching input u is a discrete variable that takes one of the three states of dc to dc buck converter switch, $\mathrm{S_w}$, namely ON, OFF and maintaining previous state. The value of the input switching status u is decided by the sliding line in the phase plane of the equation [Biswal, (2011)], [Tudoroiu, (2012)]:

$$S = c_1 x_1 + c_2 x_2 = c_1 x_1 + c_2 \frac{dx_1}{dt} = 0 \tag{17}$$

that passes through the origin (0,0), as a stable operating point for dc Buck converter. This line is like a boundary that splits the phase plane into two regions, each region being specified with a switching state to direct the system phase trajectory toward the sliding line (commutation or switching line) [Biswal, (2011)], [Tudoroiu, (2012)]. Anytime the phase trajectory reaches and tracks the sliding line converging toward the origin:

$$x_{1\infty} = 0, x_{2\infty} = 0 \text{ , when } t \overset{\Delta}{\rightarrow} t_{final}(\infty) \tag{18}$$

the system is in stable state that corresponds to an equilibrium state (stationary point, solution of the system of equations (14)).

The dynamics of the system in sliding mode is described by the previous equation of the sliding line in phase plane, and anytime if the existence and reaching conditions of the sliding mode are satisfied, a stable system is obtained [Biswal, (2011)], [Tudoroiu, (2012)]. Also, to guarantee that the system tracks the sliding surface, the control law will be defined as:

$$u = \begin{cases} 1, & S_w = ON \text{ , } S > k \\ 0, & S_w = OFF \text{ , } S < -k \\ previous \quad state \text{ , } otherwise & (-k \le S \le k) \end{cases} \tag{19}$$

where the gain k is an arbitrarily small value, one of the tuning parameters. The reasoning for choosing S as in (17) is justified by the fact that the switching boundary is to introduce a hysteresis band which determines the switching frequency of the dc buck converter.

More precisely, if the parameters of state variables are such that $S > k$, the switch $\mathrm{S_w}$ of the buck converter will turn ON, and if $S < -k$ it will turn OFF. In the band hysteresis region, for which $k \le S \le k$, the switch remains in its previous state that prevents the SMC from operating at a high frequency, and also reduces the chattering effect which induces extremely high frequency switching [Biswal, (2011)], [Tudoroiu, (2012)]. The switching conditions given by the control law (19) are depicted graphically in figure 20.

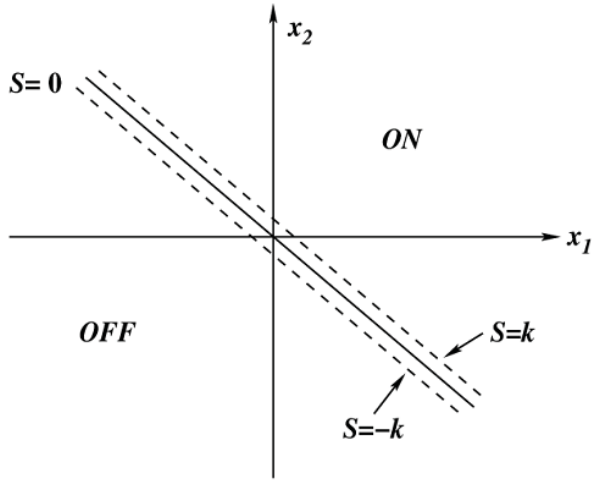

Fig. 20. Sliding line in the phase plane (x_1, x_2) ((Reproduced from [Biswal, (2011)], [Tudoroiu, (2012)])

The control law derived above provides only the information that the system trajectory is driven toward the sliding line. In order to guarantee that the trajectory is maintained on the sliding line, the existence condition of sliding mode operation, derived from Lyapunov's asymptotic stability condition, has to be satisfied [Biswal, (2011)], [Tudoroiu, (2012)]. Well, we don't enter in more details concerning the geometrical aspects of the sliding lines, the regions of the existence stability conditions, the equilibrium stable points, and so on, because is beyond the purpose of our paper, these aspects are well explained by extensive simulations in [Biswal, (2011)], [Tudoroiu, (2012)]. The following values of the system parameters and sliding coefficients we consider in our approach [Tudoroiu, (2012)]:
$v_{in} = 24\ [V], v_o = 10[V]$ (desired output voltage), Inductance of the low pass filter coil, L = 3e-3[H], Capacitance of the low pass filter, C = 47e-6[F].

To check the SMC robustness to load changes, we assume the following minimum and maximum values for load resistance [Tudoroiu, (2012)]:
R_{min} = 8 Ω, R_{max} = 20Ω, c_1 = 5, and c_2 = 0.001, Buck converter switching frequency $f_s = 100\ kHz$ (the cycle period T_s = 0.00001 seconds).

We remark also the presence of the second point of coordinates $(V_{ref}, 0)$ toward converge the control system trajectories when S_w is open, point that is called off state equilibrium point. On the sliding line, S = 0, that covers both the ON state and OFF state regions, the sliding mode occurs only on a certain portion since the phase trajectory could leave it anytime, entering for a while into one of the two outside regions. The AnyLogic model of the SMC integrated structure is presented in figure 21. The simulation results, the entry actions and the transitions are shown in detail, for SMC control strategy, in figure 22 [Tudoroiu, (2012); Tudoroiu et al., (2015a); Tudoroiu et al., (2015b)]. The selection of the parameters values for dc buck converter and sliding mode controller (the

coefficients c_1, c_2) has a great impact in the phase plane on the system phase trajectories, on the slope of the sliding line, as well as on the hysteresis region, as shown in figures 23-24 [Tudoroiu, (2012); Tudoroiu et al., (2015a); Tudoroiu et al., (2015b)]. For different combinations of the parameters values we get completely different results, even divergence for the system trajectories. The states and the transitions of the dc buck converter are defined easily in AnyLogic editor in the Properties section of the Main active object.

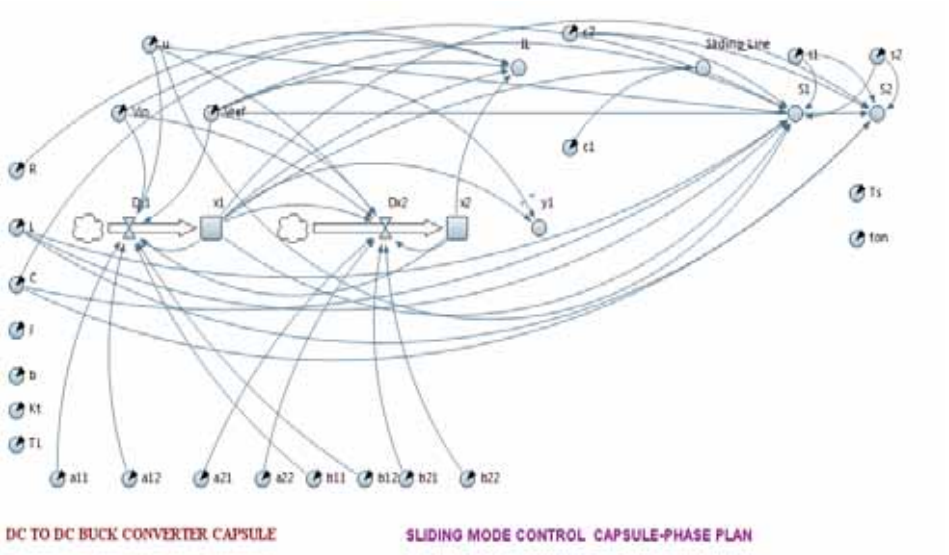

Fig. 21. Integrated structure dynamics of dc buck converter and SMC capsules- phase plan representation (Reproduced from [Tudoroiu, (2012)]).

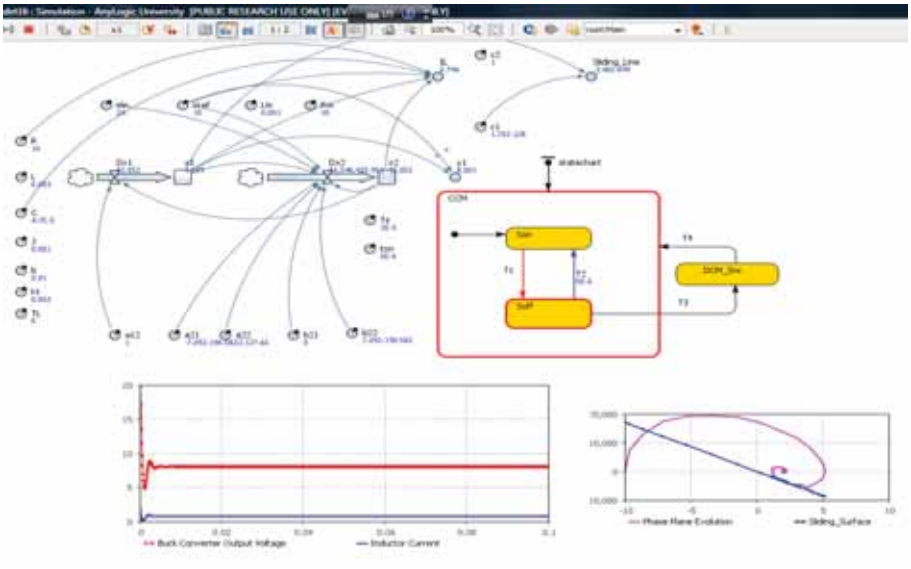

Fig. 22. Phase plane evolution of integrated structure dynamics for T_s = 1e-5[s], t_{on} = 0.5 T_s, C = 47e-6 [F],c_1 = 0.2/(RC), c_2 = 1, the existence region of stability (Reproduced from [Tudoroiu, (2012)]).

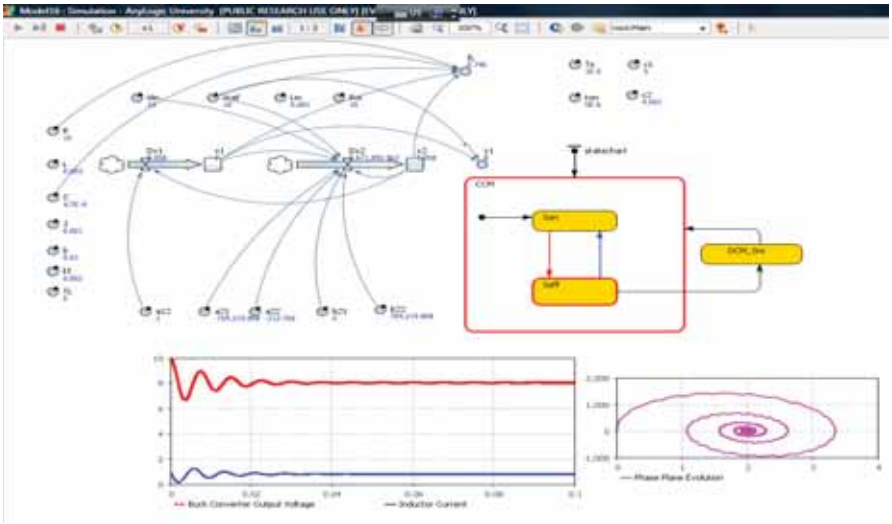

Fig. 23. Phase plane evolution for Ts = 1e-5[s], ton = 0.4Ts, C = 47e-6F (Reproduced from [Tudoroiu, (2012)]).

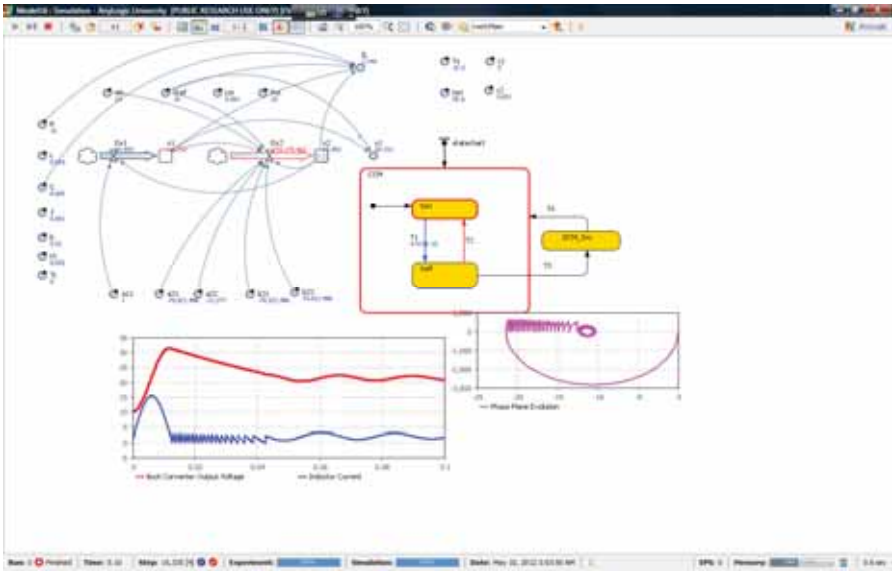

Fig. 24. Phase plane evolution for T_s = 1e-5 [s], $t_{on} = 0.5T_s$, C = 47e-6 [F] (Reproduced from [Tudoroiu, (2012)])

6. Conclusion

In this paper is simulated the sliding mode controller (SMC) embedded with dc Buck converter control system structure to stabilize and regulate the converter output voltage, despite the load current changes and unregulated power supply input voltage. The hybrid control strategy is conceived, then modeled and simulated in the same AnyLogic 6.7 University hybrid simulator Sliding mode controller (SMC) are well known by its advantages such as robustness to the load current and input power supply voltage changes, as well as by its stability. The main drawback of the control strategies is that their overall performance is dependent on the switching frequency of the network switch, excessive high switching frequency resulting in severe electromagnetic interferences (EMI) and switching losses.

Acknowledgments

We wish to express our gratitude xjtek company (available online on the website: www.xjtek.com/) to provide us the free evaluation academic version software package AnyLogic 6.7 for modeling and implementing our proposed control strategies developed in this research.

References

Biswal, M. (2011): Control Techniques for dc to dc buck converter with improved performance, Master Thesis, http://www.ethesis.nitrkl.ac.in/2976/1/Thesis.pdf

Gambier A. (2004): Real-time Control Systems: A Tutorial, http://www.ascc2004.ee.mu.oz.au/proceedings/papers/P150.pdf

Secchi, C.; Bonfe, M.; Fantuzzi, C. (2007): On the use of UML for modeling mechatronic systems, IEEE Transactions on Automation Science and Engineering, **4**(1), pp.105-113.

Selic, B., Rumbaugh, J., (1998): Using UML for Modeling Complex Real-Time Systems, pp.1-22, http://www.dcc.ttu.ee/LAP/ISP0011/umlrt.pdf

Selic, B. (2000): A generic framework for modeling resources with UML. Computers Journal, **33**(6).

Tudoroiu, R-E. (2005): Software process modeling: Investigations using the rational unified process, Master Thesis, Concordia University, Canada.

Tudoroiu, R-E. (2012): Conceiving and Implementing Applications using "Real-Time UML, PhD Thesis, Cluj-Napoca Technical University, Romania.

Tudoroiu, R-E., Astilean, A., Letia, T., Iliasi, N., Tudoroiu, N., Burdescu, D.(2015): Wireless UML-RT Simulator for Modeling and Implementing Dynamics Hybrid Structure of a Real Time PI DC Motor Control System, The Journal of Economics and Technologies Knowledge (JETK), **1**(4), pp.69-81.

Tudoroiu, R-E., Astilean, A, Letia, T., Cretu, V., Iliasi, N., Tudoroiu, N., (2015): UML-RT Simulator for Modeling and Implementing Hybrid Structure Dynamics of a Real Time PID DC Servomotor Position Control System Strategy, The Journal of Economics and Technologies Knowledge (JETK), **1**(5), pp. 68-77.